Ultrasound Biomicroscopy Imaging for Monitoring Progressive Trypsin Digestion and Inhibition in Articular Cartilage

Q Wang[1], YP Zheng[1, 2]

[1] Department of Health Technology and Informatics, [2] Research Institute of Innovative Products and Technologies, The Hong Kong Polytechnic University, Hong Kong, China

Running Title: Ultrasonic Monitoring of Cartilage Trypsin Digestion

* Correspondence address:

Dr. Zheng Yongping

Department of Health Technology and Informatics

The Hong Kong Polytechnic University

Kowloon

Hong Kong SAR, China

Tel: 852-27667664

E-mail: ypzheng@ieee.org

Submitted to: **Ultrasound in Medicine and Biology**

1st Submission: Sep 22 2008

1st revision: Jan 15 2009

2nd revision: Apr 6 2009

Abstract

This study reports an ultrasound biomicroscopy (UBM) imaging approach to monitor the progressive trypsin-induced depletion of proteoglycan (PG) and its inhibition in articular cartilage. Three fresh, normal bovine patellae were obtained, and four full-thickness cartilage-bone specimens were prepared from the lower medial side of each patella. One sample was used as a control and the other three were divided into three groups: Groups A, B, and C (n=3 for each group). After a 40 min 0.25% trypsin digestion, samples from Group A were continuously digested in trypsin solution, while those in Groups B and C were immersed in physiological saline and fetal bovine serum (FBS), respectively, for another 280 min. The trypsin penetration front was observed by UBM, and M-mode images were acquired using 50 MHz focused ultrasound and custom-developed software. The results show that the 40 min trypsin digestion degraded nearly the whole surface layer of the cartilage tissue. Further digestion in trypsin or residual digestion in saline for 280 min depleted most of the PG content, as observed in Groups A and B. The replacement of trypsin with a physiological saline solution only slightly slowed the digestion process (Group B), while trypsin inhibitors in FBS stopped the digestion in approximately 1.5 h (Group C). The normalized digestion fractions of the digested tissues were calculated from ultrasound data and histology sections, and then compared between the groups. Without the use of FBS, 80-100% of the full thickness was digested, while this number was only approximately 50% when using FBS. Our findings indicate that the UBM imaging system could provide 2-D visual information for monitoring progressive trypsin-induced PG depletion in articular cartilage. The system also potentially offers a useful tool for preparing cartilage degeneration models with precisely controlled PG depletion.

Keywords: Articular cartilage; Ultrasound; High frequency ultrasound; Ultrasound biomicroscopy; Proteoglycan depletion; Trypsin digestion; Trypsin inhibitors; Osteoarthritis

INTRODUCTION

Articular cartilage (artC) is a low frictional, load-bearing soft tissue that provides almost frictionless support for several joints. The material composition of artC is a multi-phase hydrated mixture mainly composed of 5–10% proteoglycan (PG), 10–20% collagen, and 60–80% water (Mow et al. 2005). Aggregating PGs are negatively charged bio-macromolecules that are enmeshed in the collagen matrix (Lai et al. 1991; Maroudas 1976). Therefore, PGs play an important role in determining the electrochemical and mechanical properties of articular cartilage, such as shear modulus (Zhu et al. 1993), compressive modulus (Qin et al. 2002; Zheng et al. 2001, 2005), swelling strain (Narmoneva et al. 1999; Wang and Zheng 2006) and swelling aggregate modulus (Flahiff et al. 2004; Narmoneva et al. 2002; Wang et al. 2007, 2008a). It has been widely reported that the loss of PGs is one of the earliest signs of osteoarthritis (OA), which is one of the most common joint diseases. Advanced stage OA is characterized by a partial or total loss of cartilage tissue and the direct contact of bone across the joint. (Armstrong and Mow 1982; Martini 2004; Sandy 2003; Torzilli et al. 1990). Early diagnosis of artC degeneration is very important for the treatment of OA. However, conventional methods using X-ray imaging can only detect very late stage OA. Most existing MRI systems do not have sufficient resolution for the assessment of artC. Conventional ultrasound scanners are not suited to the direct study of OA, as their resolution is also usually insufficient to image changes in artC. Further, it is difficult to scan the whole articulating surface with an ultrasound probe located outside the body. New approaches using arthroscopic imaging can provide more information about artC degeneration processes such as surface fibrillation, but it remains challenging to assess early stage OA

using video inspection. In order to evaluate new therapies such as mosaic plasty, cultured chondrocyte transplantation, and even the use of tissue-engineered cartilage, it is necessary to develop sensitive assays of the therapeutic outcome (Detterline et al. 2005; Fu et al. 2003). During the last decade, various techniques have been developed for this purpose, including mechanical indentation (Toyras et al. 2001), quantitative ultrasound (Saied et al. 1997; Joiner et al. 2001; Hattori et al. 2003; Nieminen et al. 2002,), ultrasound combined with indentation (Zheng and Mak 1996; Suh et al. 2001; Laasanen et al. 2002), water-jet indentation (Lu et al. 2009), compression (Zheng et al. 2004a), osmotic loading (Wang et al. 2008a), optical coherence tomography (OCT) (Herrmann et al. 1999), air-jet OCT indentation (Huang et al. 2009), and electromechanical measurement (Legare A et al. 2002).

Various in-vitro and in-vivo animal models mimicking human articular cartilage degeneration have been reported in the literature. These models are intended to aid the development of new diagnostic approaches and the investigation of the mechanism of degeneration. To study how the loss of PGs results in changes in morphological, biomechanical, acoustic, and bioelectrical parameters, many studies have treated normal articular cartilage with enzymes such as trypsin. Such treatment depletes PGs, mimicking natural cartilage degeneration (Basser et al., 1998; Brown et al., 2007; Deng et al., 2007; Disilvestro and Suh, 2002; Harris et al., 1972; Hunziker and Rosbenberg 1996; Laasanen et al., 2002; Moody et al., 2006; Nieminen et al., 2002; Qin et al., 2002; Saarakkala et al., 2004; Suh et al., 2001; Toyras et al., 2002; Zheng et al., 2001, 2004). In terms of the understanding of how the loss of PGs affects different physical parameters of cartilage, tremendous achievements have been made using these trypsin-treated

animal and human cartilage models. In spite of these advances, one fundamental problem in preparing these models has not been solved: how to quantify the degree of PG depletion during the trypsin treatment. In other words, how can we prepare a cartilage degeneration model with exactly the required degree of PG depletion?

The conventional way to quantify PGs in cartilage is to use histological assays by binding different stains, such as safranin-O, toluidine blue, hematocylin and eosin (H&E), and alcian blue, to differentiate different compositions in cartilage (Lyons et al. 2006). However, this method is time-consuming and invasive since it involves specimen collection, fixing, staining, slicing, imaging, and analyzing. In many studies, pilot tests are used to determine the degree of PG depletion under a certain concentration of trypsin, operating temperature, and period of treatment. Since variations in the cartilage thickness and in the distribution of PGs and chondrocytes are commonly observed between different specimens (Moody et al. 2006), it is difficult to control the trypsin digestion process using histological techniques to create calibration standards. An alternative method is to conduct histological examination after completing all necessary (nondestructive) tests on the trypsin-treated cartilage specimen, so as to quantify the PG depletion level of each specimen. This is time-consuming and, in many cases, the histologically examined PG depletion level may not be the level expected for the experimental design. Unfortunately, at that point, it is too late to alter the experiment based on this knowledge. Therefore, it is very important to have a real-time monitoring approach for preparing cartilage degeneration models with a defined PG depletion level. Furthermore, enzyme inhibitors such as fetal bovine serum (FBS) are commonly used to stop trypsin

digestion at a certain PG depletion level (Xiang et al., 2006). Using routinely available methods, it is not possible to determine precisely how long it takes for FBS to stop the trypsin digestion process or how the inhibition process proceeds, though it has been estimated in previous studies that a FBS solution can stop trypsin digestion within approximately one hour (Qin et al., 2002; Rieppo et al., 2003). In addition, although washing with saline after trypsin treatment is a very commonly used technique in the literature, we do not know whether replacing the trypsin solution with a saline solution can stop the digestion process.

Inspired by the reduction of elasticity of articular cartilage with depletion of PGs, a novel technique using high frequency ultrasound to monitor the process of trypsin digestion has been recently reported (Toyras et al., 2002; Nieminen et al. 2002; Zheng et al. 2004b; Wang et al. 2008b). The fundamental principle of this technique is that the reduction in the elasticity of PG-depleted cartilage leads to a decrease in its acoustic impedance and, thus, creates an artificial acoustic interface between the digested and undigested cartilage tissues. An ultrasound echo can be generated at this interface, and this echo shifts as the trypsin digestion progresses deeper into the tissue. With continuous recording of ultrasound signals, the trace of digestion can be viewed in an M-mode ultrasound image. This novel technique allows real-time monitoring of the process of PG depletion induced by trypsin digestion, though the reported works are still very preliminary. These earlier studies were mainly focused on the feasibility of this technique (Toyras et al., 2002; Nieminen et al. 2002; Zheng et al. 2004b). The digestion speed of a certain concentration of trypsin in cartilage was recently reported (Wang et al. 2008b). In these studies, the ultrasound beam was focused at a single location in

the articular cartilage. Thus, it is difficult to get an accurate digestion profile and it is not known whether the digestion process is site-sensitive. Furthermore, no study has been reported that monitors the trypsin inhibition process, an important step in preparing OA models with different degeneration levels.

In the present study, we test the feasibility of ultrasound biomicroscopy (UBM) imaging, or "acoustic microscopy" (Foster et al., 2000; Saijo and Chubachi 2000) for monitoring the progressive trypsin digestion process along the digestion front, as well as the inhibition process of FBS against trypsin. To investigate the inhibition efficiency of FBS against trypsin, we also examined residual trypsin digestion in physiological saline. Instead of monitoring the cartilage tissue at a single location as was done in earlier works, UBM provides a real-time, continuous view of the digestion front on the entire cross-section of the cartilage. The results obtained in this study could help in understanding the interaction between trypsin and its inhibitors. If proved feasible, UBM imaging would qualify as a useful tool for future studies involving the examination of the diffusion of different solutes, including enzymes and their inhibitors, in articular cartilage.

MATERIALS AND METHODS

Specimen preparation

Three fresh mature bovine patellae without apparent lesions were obtained from a local butcher shop within 6 hours of slaughter, and were stored at -20°C until further preparation. For each patella, four cartilage-bone plugs were prepared from the lower medial side using a

metallic punch with a diameter of 6.35 mm (Fig. 1). One of these samples was be used as a control, and the other three divided into three groups (A, B, and C) for trypsin treatment. The experimental protocols for each group are described in subsequent sections. The prepared cartilage-bone plugs were wrapped in wet gauze soaked with physiological saline and stored at -20°C until the experiment.

The ultrasound biomicroscopy (UBM) system

The ultrasound signals backscattered from the cartilage sample were acquired using a UBM system similar to the ultrasound system described in our previous reports (Wang and Zheng, 2006; Zheng et al., 2006). The UBM system, as shown in Fig. 2a, comprised a nominal 50 MHz focused ultrasound transducer (Model PI50-2, Panametrics, Waltham, MA, USA), a pulser/receiver (Model 5601A, Panametrics, Waltham, MA, USA), a 500 MHz 8-bit A/D converter (Model CompuScope 8500PCI, Gage, Canada), and a computer with custom-designed software. The transducer had a focal length of 12.7 mm, a diameter of 6.35 mm, a -6 dB beamwidth of 0.1 mm, and a -6 dB focal zone depth of 0.95 mm. The system was equipped with a 3-D translating device (Parker Hannifin Corporation, Irvine, CA, USA), which was used to adjust the position of the transducer and to drive the transducer to scan the specimen. The scan length was 6.8 mm with a displacement step of 50 μm along the specimen diameter. These conditions allowed acquisition of 2-D UBM images of the tissue in approximately 60 sec (Fig. 2). The UBM images displayed the echoes reflected from the saline-cartilage interface and the cartilage-bone interface, as well as those scattered from the cartilage tissue (Fig. 2b). Each UBM image was formed by 137 lines of A-mode ultrasound

signals, the amplitude of which corresponded to the grey levels in the image. The baseline of the radiofrequency (RF) ultrasound signal, i.e., zero magnitude, corresponded to grey level 128 out of 256. A brighter pixel in the image represents a more positive magnitude and a darker pixel represents a more negative magnitude. Fig. 3 shows the interface of the custom-developed software, in which a UBM image, the A-mode ultrasound RF signals, and an M-mode image are simultaneously displayed. The assignment of grey levels for different signal magnitudes was the same as that used for forming the UMB image.

Ultrasound examination

Before testing, the frozen cartilage-bone specimen was thawed in physiological saline solution (0.15 M NaCl) for three hours at room temperature (25±1°C). The sample was then installed in the container, and the outer ring of the cartilage surface was gently covered using rubber gel (Blu-Tack, Thomastown, Australia). This gel allowed trypsin or serum to penetrate into the sample only from the surface layer toward the cartilage-bone interface (Fig. 2a).

After the specimen equilibrated in physiological saline, ultrasound examination was performed in two phases. In the first phase, the saline solution was removed from the container using an injection syringe and quickly (within 30 seconds) replaced with the trypsin solution (0.25%, Cat. No. 25200-056, GiBCO, Invitrogen Inc. Burlington, ON, Canada). The progressive digestion of all specimens from Groups A, B, and C was monitored by the UBM system for 40 minutes. In the second phase, the specimens of Group A were continuously immersed in the trypsin solution, while the trypsin solution in Group B and Group C was

removed within 30 seconds and replaced with physiological saline and fetal bovine serum (Cat. No. 16000-036, GiBCO, Invitrogen Inc. Grand Island, NY, USA), respectively. We refer to these two processes as the residual trypsin digestion in physiological saline and the inhibition in FBS. This phase lasted for 280 minutes.

In M-mode images, markers were manually inserted at an interval of approximately 5 min along the inclined trace (see Fig. 3 M-mode Display). This trace represents the process of trypsin degradation of the PGs, or the interaction between trypsin and its inhibitors. According to the locations of these markers, the software automatically interpolates the curve representing the depth of trypsin digestion as a function of time. This procedure was repeated six times for each specimen at different locations along the center of the 2-D cross-sectional image to obtain 6 different interpolation curves. These curves were then averaged to reduce possible site variance of the digestion and to smooth the trace. The variation among the 6 digestion traces of each individual specimen was tested by calculating the root mean square (RMS) difference with respect to the averaged trace. The average curve was used for estimation of the digestion fraction (the digestion depth normalized to the cartilage full-thickness). These normalized values were used for comparison between the ultrasonic and histological measurements, as the normalization can reduce effects caused by variations of ultrasound speed between different cartilage samples and potential shrinkage of the specimen during the process of histological analysis. The averaged digestion traces obtained for the 3 individual samples for each group were further averaged, and their RMS differences were also calculated, to examine the variation among samples.

In this study, the full thickness of the cartilage layer and the digestion depth were calculated using a previously described method (Zheng et al., 2002). The cartilage thickness measurement was based on the estimation of the time-of-flight between the echoes reflected from the cartilage surface and the cartilage-bone interface. A cross-correlation technique was used to match echoes. Since the use of a constant sound speed in both healthy and PG-depleted cartilage causes an overestimation in the measurement of cartilage thickness (Pellaumail et al., 2002), sound speeds of 1675 m/s and 1668 m/s were taken for the normal and PG-depleted cartilage tissues, respectively (Nieminen et al., 2002; Patil et al., 2004).

Histology

After ultrasound examination, all control and trypsin-treated specimens were fixed in a buffered formalin solution (10%), decalcified in a 10% EDTA solution using an ultrasound method reported by Guo et al. (2007), then embedded in paraffin. The central region of the specimen was serially sectioned using a rotary microtome (Leica RM-2135, Cambridge, UK). The 4 μm-thick deparaffined sections were stained with safranin O (Cat. No. F7258, SiGMA, MO, USA) and contra-stained with fast green (Cat. No. S-2255, SiGMA, MO, USA). The sections were viewed with an imaging system comprising a microscope (Model FN-S2N, Nikon, Japan) and a digital camera (DXM 1200X, Nikon, Japan). In the optical micrographs, red color due to safranin O indicates the presence of PG (Leung et al. 1999; Qin et al. 2002). The depth of the trypsin-digested zone was estimated by measuring the depth of the fast green-stained zone in the histological image. To obtain the digested fraction, the digestion

depth was normalized by the full cartilage thickness, measured from the cartilage surface to the interface between the deep cartilage layer and the bone. The 3 digestion fraction values obtained from 3 sections for each specimen were averaged, and the mean value was compared with the ultrasound measurement.

RESULTS

Fig. 4 shows UBM images at the central sample section collected after 0 min, 40 min, 2 h, and 4 h of trypsin digestion of three cartilage samples from Groups A, B and C. As the trypsin penetrated into the cartilage tissue and broke down the aggregating PGs, an interface between the digested and undigested tissues was generated due to the change in the acoustic impedance of the PG-depleted tissue. Consequently, an additional ultrasound echo appeared. As digestion continued, this interface moved deeper into the tissue (Fig. 4). In the first phase of this study, we observed that the 40 min trypsin treatment digested approximately 30-40% of the full thickness of the cartilage (Fig. 4b, f, j). In the second phase, the digestion of Group A continued until, after 2 h of trypsin digestion, the interface was close to the bone (Fig. 4c). The digestion front reached the bone and disappeared after 4 h of digestion (Fig. 4d). For Group B, the digestion front continued to shift down into the deep layer even after trypsin was replaced with physiological saline (Fig. 4g, h). In Group C, trypsin was replaced with FBS, which contains trypsin inhibitors. Although this replacement is supposed to stop trypsin digestion, the digestion front (Fig. 4k) kept moving deeper after 2 h of inhibition, as compared to the front in Fig. 4j. Between 2 h and 4 h of inhibition (Fig. 4k and Fig. 4l), the digestion front entered a static phase and moved little. As seen in Fig. 4, the digestion level of Groups A

and B was much deeper than that of Group C.

The results demonstrate that the digestion trace extracted from the M-mode image was rather repeatable among the 6 traces for a single specimen, and among the traces of the three specimens in each group. The averaged root mean square (RMS) variations (with respect to the corresponding averaged traces) were 5.1±1.5% for a single specimen and 7.4±3.0% among the three specimens. By analyzing the inclined digestion traces in the M-mode images from different groups (Fig. 5), we found that the pattern of residual trypsin digestion experienced by Group B was similar to the trypsin digestion pattern of Group A, but different from the inhibition process of Group C. In the second phase of the study, i.e., after the first 40 min trypsin digestion, we measured the digestion depth and plotted it as a function of time for the three groups (Fig. 6). Since no more trypsin entered into the tissue, the residual digestion of Group B in physiological saline slowed down in comparison to the continuous trypsin digestion in Group A. Approximately 0.8 mm and 0.6 mm of cartilage were digested after 280 min for groups A and B, respectively. Group C underwent a digestion process similar to Groups A and B during the first 50 min, when the trypsin inhibitors might have not penetrated into the tissue. After that time, the inhibitors started to affect the function of trypsin. This inhibiting process lasted for approximately one hour (Fig. 6), until the movement of the digestion front stopped. The final digestion depth for Group C was approximately 0.3 mm.

We calculated the digestion fractions from histological sections of the specimens in the control group and groups A, B, and C and compared these with the results of the ultrasonic

measurements (Fig. 5, Table 1). The results reveal that all or almost all of the PGs in the entire cartilage layer were digested by the 280-minute trypsin digestion and by the residual digestion. FBS effectively stopped trypsin digestion at the middle layer, while physiological saline only slightly weakened the trypsin digestion in the cartilage. According to Table 1, the results of the ultrasonic and histological measurements on the digested portion of the trypsin-treated articular cartilage did not agree well for specimens treated only by trypsin, or for those treated with trypsin and serum. The results of the specimens treated with trypsin and saline did agree well.

DISCUSSION

In this study, we observed in real-time the penetration of trypsin digestion and the process of FBS inhibition using UBM cross-sectional images as well as M-mode ultrasound images. We performed both imaging techniques by detecting the additional echoes reflected from the interface between the digested and undigested tissues. The enzyme digestion front moved vertically from the surface layer to the deeper layer with long digestion times. Among the three specimen groups tested, the overall process of trypsin digestion was similar within the first 40 min. Further digestion in trypsin, residual digestion in saline, and inhibition of digestion in FBS gave consistent results within the 3 specimens tested for each group, with an RMS deviation of 7.4±3.0%. However, we observed differences between the specimens in the profile of the digestion front, the magnitude of the interface echo, and the depth of the digestion front at a given time. This finding agrees with the results of a recent study that also reported variations in trypsin digestion between different specimens (Moody et al., 2006).

Most importantly and interestingly, we found that the digestion front in the tissue section was not a straight line. This finding indicates that either the distribution of the PGs or the diffusion rate of trypsin along the depth direction varied from site to site, even in a cartilage disc with a diameter of only 6.35 mm. Our histological images also showed that the interfaces between the safranin O-stained and fast green-stained areas were not exactly horizontal for all specimens. This inhomogeneity of tryspin digestion further demonstrates the inhomogeneous distribution of PGs and other components in cartilage tissue. The results also confirm the necessity of using 2-D imaging to monitor the digestion and inhibition process, as the single-location monitoring reported in earlier studies may not give a complete description of the digestion front (Toyras et al., 2002; Nieminen et al. 2002; Zheng et al. 2004b; Wang et al. 2008). Although the sides of the cartilage specimens were sealed with a rubber gel, it might be still possible that the trypsin solution diffused into the cartilage tissue from the sides. This possibility may explain why the interface echo was relatively weak or disappeared towards the two sides of the cross-sectional image, as observed in the images of Fig. 4. Further studies may be warranted to systematically investigate the lateral diffusion of trypsin solution from the sides of specimens. 3-D ultrasound imaging of articular cartilage may provide even more insight and direct information about what occurs in the tissue during progressive degeneration. Early studies have attempted 3-D imaging of articular cartilage with morphological lesions or topographic changes due to OA (Cashman et al., 2002; Gaddipati et al., 2004; Lefebvre et al., 1998). Methods have also been developed to attempt to provide 3-D information about effects of drugs on articular cartilage (Jaffre et al., 2003). However, little work has been done to provide real-time 3-D imaging of degeneration processes in articular cartilage. Using 3-D

ultrasound imaging techniques to display the progressive degeneration of articular cartilage should be the subject of further study.

Besides studying the digestion process, we also investigated the inhibiting effect of FBS against trypsin digestion using UBM in this study. It has been reported that a FBS solution can stop trypsin digestion within approximately one hour (Qin et al., 2002; Rieppo et al., 2003). In our study, it took about one and half hours for FBS to totally inhibit digestion at a trypsin concentration of 0.25%. In addition to the time required for inhibition, we have also reported, for the first time, the process of FBS inhibition, which is rather consistent among the three specimens. In the future, it would be very interesting to study what affects the inhibition process, and what the differences are between articular cartilage tissue from different species.

Using UBM, we monitored trypsin digestion, residual digestion in physiological saline, and the inhibition process of FBS, and revealed the differences between the three processes. Our results show that the 40 min trypsin-digested specimens continued to be digested by residual enzyme in the tissue. Replacement of the external solution with saline solution appeared to have little influence on this digestion. Therefore, using enzyme inhibitors is necessary to minimize the residual enzyme digestion effect (~0.6 mm further penetration in 280 min) to achieve a more accurate assessment of the degeneration level of the specimens. Use of inhibitors will also increase the accuracy of subsequent biomechanical or acoustic measurements. It should be noted that, despite the use of a digestion inhibitor, the digestion depth increased approximately 0.2 mm (Fig. 6) during the inhibition process of FBS. This

result should be taken into account when using FBS as an inhibition solution. It would very interesting to further investigate the inhibition process of other types of trypsin inhibitor solutions. The potential of this ultrasound method to monitor the diffusion process of other solutes in articular cartilage, such as those studied by MRI techniques (Burstein et al., 1993; Xia et al., 1995; Woertler et al., 2004), could also be explored in future studies. In our earlier studies, we have demonstrated that the diffusion of salt (NaCl) between cartilage and the bathing solution can be monitored using real-time ultrasound. This monitoring is accomplished by measuring changes in the speed of sound and osmotic swelling in cartilage (Zheng et al. 2004b; Wang and Zheng 2006; Wang et al. 2007, 2008). Using MRI or radioisotope marking techniques, the target molecules are directly monitored by their MR or radiation features. In this ultrasound method, the target molecules are indirectly monitored through changes in the morphological or acoustic features of the tissue induced by the target molecules during diffusion. If the feasibility of this ultrasonic approach can be more systematically demonstrated in future studies, it may potentially provide a more accessible technique for monitoring various solute transport processes in cartilage and, potentially, other tissues.

The finding that residual digestion progresses in saline partially explains the disagreement we noted in an earlier study between the trypsin digestion depths measured by ultrasound and histology (Wang et al. 2008b). With the residual digestion in saline taken into account in the calculation of the digested portion, the results obtained in this study by histology and ultrasound agree very well for all three cartilage specimens (0.84±0.22 vs. 0.83±0.19).

However, for the three specimens treated solely by trypsin for 40 + 280 min, the digested portion measured with histology was larger than that obtained by ultrasound (0.96±0.07 vs. 0.88±0.06). This difference can still be explained by residual digestion after the termination of the experiments. Even though the specimen has not been put in saline solution after the trypsin treatment, the trypsin in the specimen may continue to degrade the sample after the end of ultrasound monitoring and removal from the trypsin solution. This residual digestion occurred after the trypsin treatment, but before the histology test. Thus, this digestion increased the value of the digestion portion measured by histology, but not the value measured by ultrasound. For the three specimens treated with trypsin followed by FBS inhibition, the digested portion measured by histology was smaller than that obtained by ultrasound (0.38±0.06 vs. 0.50±0.02). One possible reason for this observation might be that some of the digestion that occurred during the inhibition process (approximately 0.2 mm, see Fig. 6) could not be detected by histology (safarin O still stained this portion red). This phenomenon might result if the PG had not been completely depleted by trypsin prior to the treatment with FBS. Such an incomplete depletion might have already reduced the tissue elasticity, affecting the acoustic impedance. However, if the fragments were not small enough to move out of the collagen network, the main components of PG, chondroitin sulphate and keratan sulphate, could still be stained red by safarin O. This explanation would account for the observed transition in color intensity (Fig. 6). Due to the extremely long experimental time for testing each specimen, we could only test 3x3 specimens in this study, and were not able to conduct any statistical analysis of these results. Future studies with more cartilage specimens would be required to draw firmer conclusions about these findings. Further efforts with more

specimens and other reference methods are also needed to confirm whether the digestion that occurred after the appearance of FBS could be viewed with safarin O staining in histology. These efforts would also confirm whether the mechanical/acoustic interface induced by the partial trypsin digestion matches the safarin O staining interface. Since the digestion front observed in ultrasound images moves only when PGs are digested deeper in the sample, we can use this ultrasound method to detect the real interface between PG-depleted and intact cartilage tissues. This ability is unaffected by whether the specimen is in trypsin, saline or inhibitor solution, and does not depend on whether the depleted PG can be viewed by safarin O staining. Furthermore, it has been reported that histological staining might not accurately reflect the total PG content in articular cartilage (Camplejohn and Allard, 1998). Considering these points, the presently-reported ultrasound method may provide not only the benefits of simplicity and real-time measurements, but possibly also increased accuracy in monitoring PG depletion in articular cartilage.

CONCLUSIONS

This study provides a useful approach to observe a dynamic digestion process inside cartilage tissue. We compared the processes of tryspin digestion, residual digestion in physiological saline, and FBS inhibition of trypsin digestion. The results show that residual digestion in physiological saline can degrade cartilage nearly as much as continuous trypsin digestion. Although FBS did stop digestion in approximately one and half hours, the digestion continued during the first 30 min of this period. Due to the labor-intensive experiments and extremely long experimental time, we could only test a limited number of specimens in this study. Future

studies with more cartilage specimens from different species could lead to more definite conclusions. This method may be used to prepare in vitro cartilage degeneration models with precisely controlled PG depletion levels, or to investigate the diffusion of various solutes, such as various enzymes or chemicals, inside articular cartilage, as long as they can induce a change in the acoustic impedance of cartilage. Such precisely controlled OA models may facilitate the development of new diagnostic tools for early degeneration of articular cartilage and the investigation of the mechanisms of cartilage degeneration.

Acknowledgements

This work was partially supported by the Research Grants Council of Hong Kong (PolyU 5245/03E, PolyU 5318/05E, PolyU5354/08E) and The Hong Kong Polytechnic University.

REFERENCES

Armstrong CG, Mow VC. Variations in the intrinsic mechanical properties of human cartilage with age, degeneration and water content. J Bone Joint Surg. 1982; 64A: 88-94.

Basser PJ, Schneiderman R, Bank RA, Wachtel E, Maroudas A. Mechanical properties of the collagen network in human articular cartilage as measured by osmotic stress technique. Arch Biochem Biophys. 1998; 351: 207-19.

Brown C P, Hughes S W, Crawford R W, Oloyede A. Ultrasound assessment of articular cartilage: Analysis of the frequency profile of reflected signals from naturally and artificially degraded samples. Connective Tissue Research. 2007; 6: 277-285.

Burstein D, Gray ML, Hartman AL, Gipe R, Foy BD. Diffusion of small solutes in cartilage as measured by nuclear-magnetic-resonance (NMR) spectroscopy and imaging. J Ortho Res. 1993;11: 465-78.

Camplejohn KL, Allard SA. Limitations of safranin 'O' staining in proteoglycan-depleted cartilage demonstrated with monoclonal antibodies. Histochemistry. 1988; 89:185-8.

Cashman PM, Kitney RI, Gariba MA, Carter ME. Automated techniques for visualization and mapping of articular cartilage in MR images of the osteoarthritic knee: a base technique for the assessment of microdamage and submicro damage. IEEE Trans Nanobioscience. 2002; 1(1): 42-51.

Deng X, Farley M, Nieminen MT, Gray M, Burstein D. Diffusion tensor imaging of native and degenerated human articular cartilage. Magn Reson Imaging. 2007; 25: 168-71.

Detterline AJ, Goldberg S, Bach BR, Cole BJ Treatment options for articular cartilage defects of the knee. Orthopaedic Nursing. 2005; 24: 361-366.

DiSilvestro MR, Suh JK. Biphasic poroviscoelastic characteristics of proteoglycan-depleted articular cartilage: Simulation of degeneration. Ann Biomed Eng. 2002; 30: 792-800.

Foster FS, Pavlin CJ, Harasiewicz KA, Christopher DA, Turnbull DH. Advances in ultrasound biomicroscopy. Ultrasound Med. Biol. 2000; 26: 1-27.

Fu FH, Musahl V. The treatment of focal articular cartilage lesions of the knee - Future trends and technologies. Sports Med Arthroscopy Review. 2003; 11: 202-212.

Gaddipati D, Stewart T, Zwicky G. Diagnosis of articular cartilage using 3-D visualization and correlation with patient data. Conf Proc IEEE Eng Med Biol Soc. 2004; 3: 1821-4.

Guo X, Zheng YP, Lam WL. Ultrasound machine assists decalcification. Calcified Tissue International. 2007; 80, S52.

Harris ED Jr, Parker HG, Radin EL, Krane SM. Effects of proteolytic enzymes on structural and mechanical properties of cartilage. Arthritis Rheum. 1972; 15: 497-503.

Hattori K, Mori K, Habata T, Takakura Y, Ikeuchi K. Measurement of the mechanical condition of articular cartilage with an ultrasonic probe: quantitative evaluation using

wavelet transformation. Clinic Biomech. 2003; 18: 553-557.

Herrmann JM, Pitris C, Bouma BE, Boppart SA, Jesser CA, Stamper DL, Fujimoto JG and Brezinski ME. High resolution imaging of normal and osteoarthritic cartilage with optical coherence tomography. J Rheumatology. 1999; 26: 627-635.

Huang YP, Zheng YP, Wang SZ, Chen ZP, Huang QH, He YH. An OCT-based air jet indentation system for measuring mechanical properties of soft tissues. Meas Sci Tech. 2009; 1: article No. 015805.

Hunziker EB, Rosenberg LC. Repair of partial-thickness defects in articular cartilage: Cell recruitment from the synovial membrane. J Bone Joint Surg (Am). 1996; 78A: 721-733.

Jaffre B, Watrin A, Loeuille D, Gillet P, Netter P, Laugier P, Saied A. Effects of anti-inflammatory drugs on articular cartilage. Arthritis & Rheumatism. 2003; 48: 1594-601.

Joiner GA, Bogoch ER, Pritzker KP, Buschmann MD, Chevrier A, and Foster FS. High frequency acoustic parameters of human and bovine articular cartilage following experimentally-induced matrix degradation. Ultrasonic Imaging. 2001; 23: 106-116.

Maroudas A. Balance between swelling pressure and collagen tension in normal and degenerate cartilage. Nature; 1976; 260: 808-809.

Nieminen HJ, Toyras J, Rieppo J, Nieminen MT, Hirvonen J, Korhonen R, Jurvelin JS. Real-time ultrasound analysis of articular cartilage degradation in vitro. Ultrasound Med Biol. 2002; 28: 519-525.

Laasanen MS, Toyras J, Hirvonen J, Saarakkala S, Korhonen RK, Nieminen MT, Kiviranta I, Jurvilin JS. Novel mechano-acoustic technique and instrument for diagnosis of cartilage degeneration. Physiol Meas. 2002; 23: 491-503.

Lai WM, Hous JS, Mow VC. A triphasic theory for the swelling and deformation behaviors of articular cartilage. J Biomech Eng. 1991; 113: 245-258.

Lefebvre F, Graillat N, Cherin E, Berger G, and Saied A, Automatic three dimensional reconstruction and characterization of articular cartilage from high resolution ultrasound acquisition. Ultrasound Med Biol. 1998; 24: 1369-81.

Legare A. Garon M, Guardo R, Savard P, Poole AR and Buschmann MD. Detection and analysis of cartilage degeneration by spatially resolved streaming potentials. J Orthopaedic Res. 2002; 20: 819-826.

Leung KS, Qin L, Leung MCT, Fu LLK, Chan CW. Decrease in proteoglycans content of the remaining patellar articular cartilage after partial patellectomy in rabbits. J Clin Exp Rheumatol. 1999; 17: 597-600.

Lu MH, Zheng YP, Huang QH, Ling C, Wang Q, Bridal L, et al. Noncontact Evaluation of articular cartilage degeneration using a novel ultrasound water jet indentation system. Ann Biomed Eng. 2009; 37: 164-75.

Lyons TJ, McClure SF, Stoddart RW, and McClure J. The normal human chondro-osseous junctional region: evidence for contact of uncalcified cartilage with subchondral bone and marrow spaces. Musculoskeletal Disorders. 2006; 7: 52-60.

Martini FH. Fundamentals of anatomy and physiology (6th Edition), Upper Saddle River, NJ: Prentice Hall, 2004.

Moody HR, Brown CP, Bowden JC, Crawford RW, McElwain DL, Oloyede AO. In vitro degradation of articular cartilage: does trypsin treatment produce consistent results? J Anat. 2006; 209: 259-67.

Mow VC, Gu WY, Chen FH. Structure and function of articular cartilage and meniscus. In: Mow VC, Huiskes R, ed. Basic Orthopaedic Biomechanics and Mechano-Biology (3rd Edition). Lippincott Williams & Wilkins, PA, USA. 2005. pp. 181-258.

Narmoneva DA, Wang JY, Setton LA. Nonuniform swelling-induced residual strains in articular cartilage. J Biomech. 1999; 32: 401-408.

Narmoneva DA, Cheung HS, Wang JY, Howell DS, Setton LA. Altered swelling behavior of femoral cartilage following joint immobilization in a canine model. J Orthop Res. 2002; 20: 83-91.

Nieminen HJ, Toyras J, Rieppo J, Nieminen MT, Hirvonen J, Korhonen R, Jurvelin JS. Real-time ultrasound analysis of articular cartilage degradation in vitro. Ultrasound Med Biol. 2002; 28: 519-25.

Patil SG, Zheng YP, Wu JY, Shi J. Measurement of depth-dependency and anisotropy of ultrasound speed of bovine articular cartilage in vitro. Ultrasound Med Biol. 2004; 30: 953-63.

Pellaumail B, Watrin A, Loeuille D, Netter P, Berger G, Laugier P, Saied A. Effect of articular cartilage proteoglycan depletion on high frequency ultrasound backscatter. Osteoarthritis Cartilage. 2002; 10: 535-41.

Qin L, Zheng YP, Leung CT, Mak AFT, Choy WY, Chan KM. Ultrasound detection of trypsin-treated articular cartilage: its association with cartilaginous proteoglycans assessed by histological and biochemical methods. J Bone Miner Metab. 2002; 20: 281-7.

Rieppo J, Toyras J, Nieminen MT, Kovanen V, Hyttinen MM, Korhonen RK, Jurvelin JS, Helminen HJ. Structure-function relationships in enzymatically modified articular cartilage. Cells Tissues Organs. 2003; 175: 121-32.

Saarakkala S, Toyras J, Hirvonen J, Laasanen MS, Lappalainen R, Jurvelin JS. Ultrasonic quantitation of superficial degradation of articular cartilage. Ultrasound Med Biol. 2004; 30: 783-92.

Saied A, Cherin E, Gaucher H, et al. Assessment of articular cartilage and subchondral bone: subtle and progressive changes in experimental osteoarthritis using 50 MHz echography in vitro. J Bone Mineral Res. 1997; 12: 1378-1387.

Saijo Y, Chubachi N. Microscopy. Ultrasound Med Biol. 2000; 26: Suppl. 1 S30-S32.

Sandy JD. Proteolytic degradation of normal and osteoarthritic cartilage matrix. In: Brandt KD, Doherty M, Lohmander LS, ed. Osteoarthritis, Oxford; New York: Oxford University Press, 2003. pp. 82-92.

Suh JKF, Youn I, Fu FH. An in situ calibration of an ultrasound transducer: A potential application for an ultrasonic indentaiton test of articular cartilage. J Biomechanics. 2001; 34: 1347-1353.

Torzilli PA, Askari E, Jenkins JT. Water content and solute diffusion properties in articular cartilage. In: Mow VC, Ratcliffe A, Woo SLY, ed. Biomechanics of diarthrodial joints (Vol. I), Springer-Verlag, New York Inc., 1990. pp. 363-390.

Toyras J, Lyyra-Laitinen T, Niinimaki M, Lindgren R, Nieminen MT, Kiviranta I, Jurvelin JS. Estimation of the Young's modulus of articular cartilage using an arthroscopic indentation instrument and ultrasonic measurement of tissue thickness. J Biomechanics. 2001; 34: 251-256.

Toyras J, Nieminen HJ, Laasanen MS, Nieminen MT, Korhonen RK, Rieppo J, Hirvonen J, Helminen HJ, Jurvelin JS. Ultrasonic characterization of articular cartilage. Biorheology. 2002; 39: 161-9.

Wang Q, Zheng YP. Non-contact evaluation of osmosis-induced shrinkage and swelling behavior of articular cartilage in situ using high-frequency ultrasound. Instrument Sci Technol. 2006; 34: 317-34.

Wang Q, Zheng YP, Niu HJ, Mak AFT. Extraction of mechanical properties of articular cartilage from osmotic swelling behavior monitored using high-frequency ultrasound. J Biomech Eng. 2007; 129: 413-22.

Wang Q, Zheng YP, Leung G, Lam WL, Guo X, Lu HB, Qin L, Mak AFT. Altered osmotic swelling behavior of proteoglycan-depleted bovine articular cartilage using high frequency ultrasound. Physics in Medicine and Biology. 2008a; 53: 2537-2552.

Wang Q, Zheng YP, Qin L, Huang QH, Lam WL, Leung G, Guo X, Lu HB. Ultrasonic assessment of progressive proteoglycan depletion of articular cartilage in real-time. Ultrasound in Medicine and Biology. 2008b; 34: 1085-1092.

Woertler K, Buerger H, Moeller J, Rummeny EJ. Patellar articular cartilage lesions: in vitro MR imaging evaluation after placement in gadopentetate dimeglumine solution. Radiology. 2004; 230: 768-73.

Xia Y, Farquhar T, Burton-Wurster N, Vernier-Singer M, Lust G, Jelinski LW. Self-diffusion monitors degraded cartilage. Arch Biochem Biophys. 1995; 323: 323-8.

Xiang J, Chiang PP, Hu Y, Smith DE, Keep RF. Role of PEPT2 in glycylsarcosine transport in astrocyte and glioma cultures. Neurosci Lett. 2006; 396: 225-9.

Zheng YP, Ding CX, Bai J, Mak AFT, Qin L. Measurement of the layered compressive properties of trypsin-treated articular cartilage: an ultrasound investigation. Med Biol Eng Comput. 2001; 39: 534-41.

Zheng YP, Mak AFT, Lau KP, Qin L. An ultrasonic measurement for in vitro depth-dependent equilibrium strains of articular cartilage in compression. Phys Med Biol. 2002; 7: 3165-80.

Zheng YP, Bridal SL, Shi J, Saied A, Lu MH, Jaffre B, et al. High resolution ultrasound elastomicroscopy imaging of soft tissues: system development and feasibility. Phys Med Biol. 2004a; 49: 3925-38.

Zheng YP, Shi J, Qin L, Patil SG, Mow VC, Zhou KY. Dynamic depth-dependent osmotic swelling and solute diffusion in articular cartilage monitored using real-time ultrasound. Ultrasound Med Biol. 2004b; 30: 841-9.

Zheng YP, Niu HJ, Mak AFT, Huang YP. Ultrasonic Measurement of depth-dependent transient behaviors of articular cartilage under compression. J Biomechanics. 2005; 38: 1830-7.

Zheng YP, Lu MH, Wang Q. Ultrasound elastomicroscopy using water jet and osmosis loading: potentials for assessment for articular cartilage. Ultrasonics. 2006; 44 Suppl 1: e203-9.

Zhu W, Mow VC, Koob TJ, Eyre DR. Viscoelastic shear properties of articular cartilage and the effects of glycosidase treatments, J Orthop Res 1993; 11: 771-781.

Figure Captions

Fig. 1 Schematic of specimen preparation and the experimental protocol.

Fig. 2 (a) Block diagram of the ultrasound biomicroscopy system. (b) A frame of an ultrasound biomicroscopic (UBM) image of an area 6.8 mm in width. The image height represents a single-way ultrasound time-of-flight of 2.05 μs, which corresponds to 3.3 mm in cartilage.

Fig.3 The user interface of the signal processing software. An M-mode image (upper left, with a scanning time of 60 s), an UBM image (upper right, representing a width of 6.8 mm) and A-mode ultrasound RF signals (lower, with a scanning depth of 3.3 mm if fully in cartilage) of articular cartilage during trypsin digestion were displayed in real-time using the custom-designed program. The grey levels of the M-mode and UBM image linearly represent the amplitude of the RF signals, with a grey level 128 out of 256 representing zero magnitude of the RF signal. The black dots in the M-mode image are the manually placed markers used for interpolation of the inclined digestion trace. The interval between markers was approximately 5 min. To avoid overlapping the trace, fewer marks than required are indicated in the figure.

Fig. 4 UBM images collected from a typical specimen of Groups A (a-d), B (e-h), and C (i-l). The samples shown in panels a, e, and i were collected at the beginning of trypsin digestion; the samples in panels b, f, and j were from the end of the 40 min trypsin digestion; the samples in c, g, and k were collected after specimens were submerged in trypsin,

physiological saline, and FBS, respectively, for 2 hours; panels d, h, and l are the UBM images after specimens were submerged in trypsin, physiological saline, and FBS, respectively, for 4 hours. In all images, the width was 6.8 mm and the scanning depth was 3.3 mm if fully in cartilage.

Fig. 5 M-mode ultrasound images and histological sections obtained at the central region of a typical specimen from Groups A (a), B (b) and C (c). M-mode images were collected during the 40 min trypsin digestion, the 280 min trypsin digestion, residual digestion in physiological saline, and the inhibition process in FBS. Solid white arrows indicate the digestion trace. Histological images on the right and left sides were collected from intact and digested specimens, respectively. The dashed line indicates the interface of the PG-depleted and PG-unaffected cartilage zone. Red staining by safranin O indicates the presence of PGs.

Fig. 6 Curves of the averaged digestion depth as a function of time for the three groups. After the replacement of trypsin with FBS, a period of approximately 1.5 hours was needed to completely stop the trypsin digestion.

Table Caption

Table 1: The mean digestion fraction of the digested samples measured at the end of the 40 min trypsin digestion and during various 280 min treatments.

1
2

Figure 1

Click here to download high resolution image

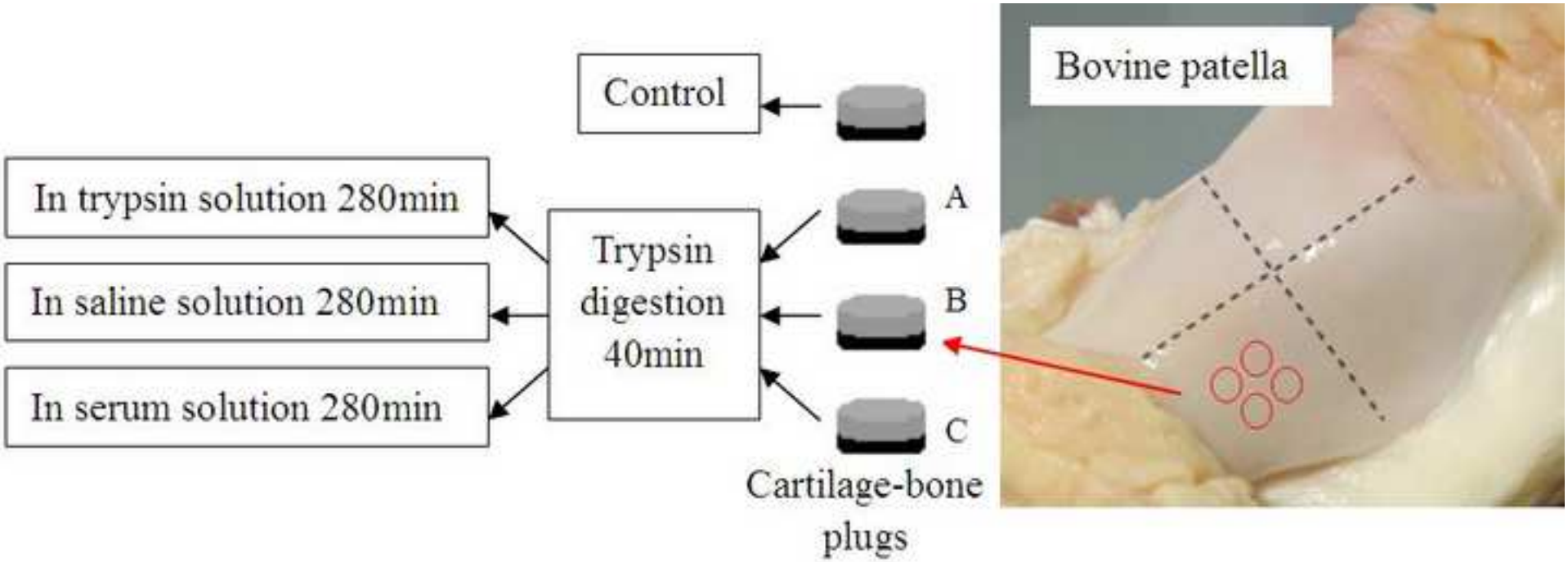

Figure 2a
Click here to download high resolution image

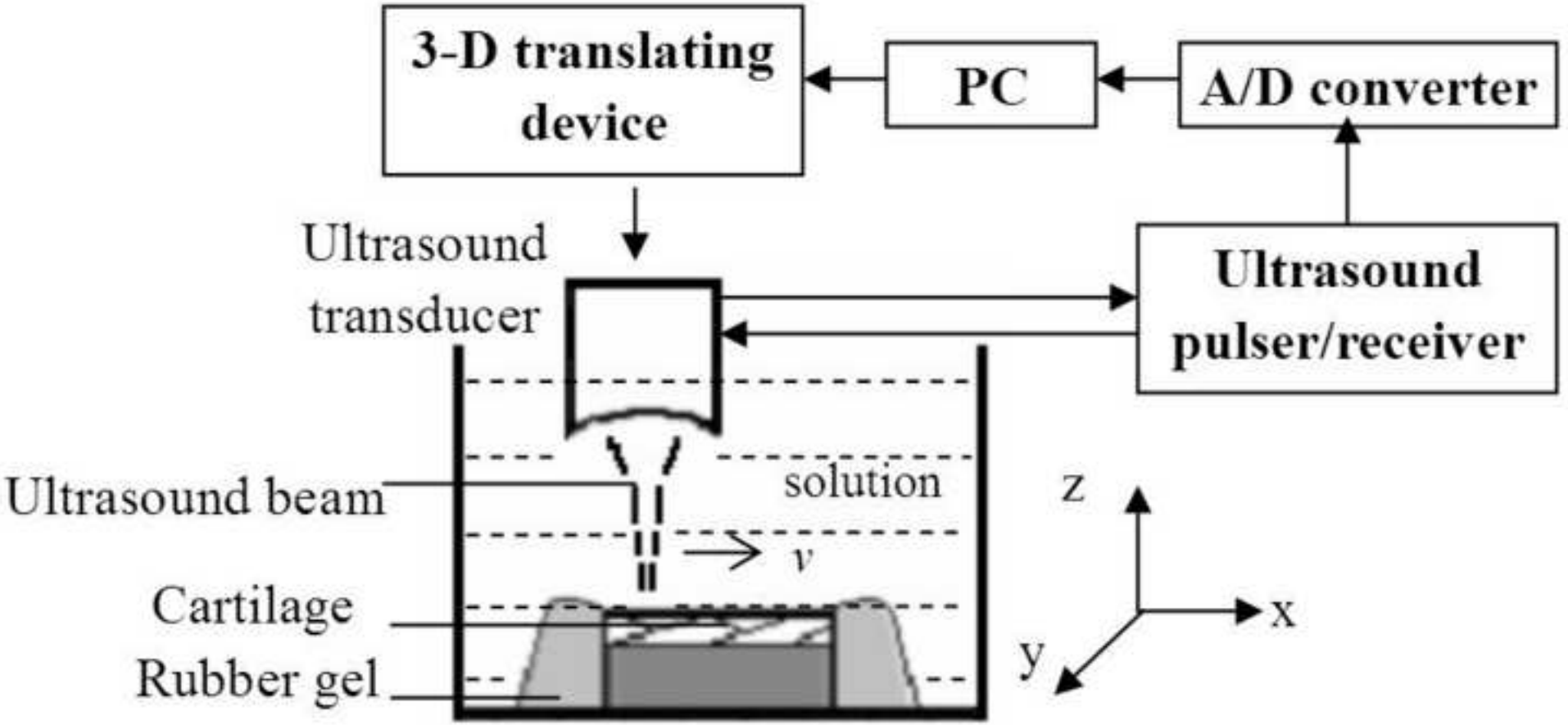

Figure 2b

Click here to download high resolution image

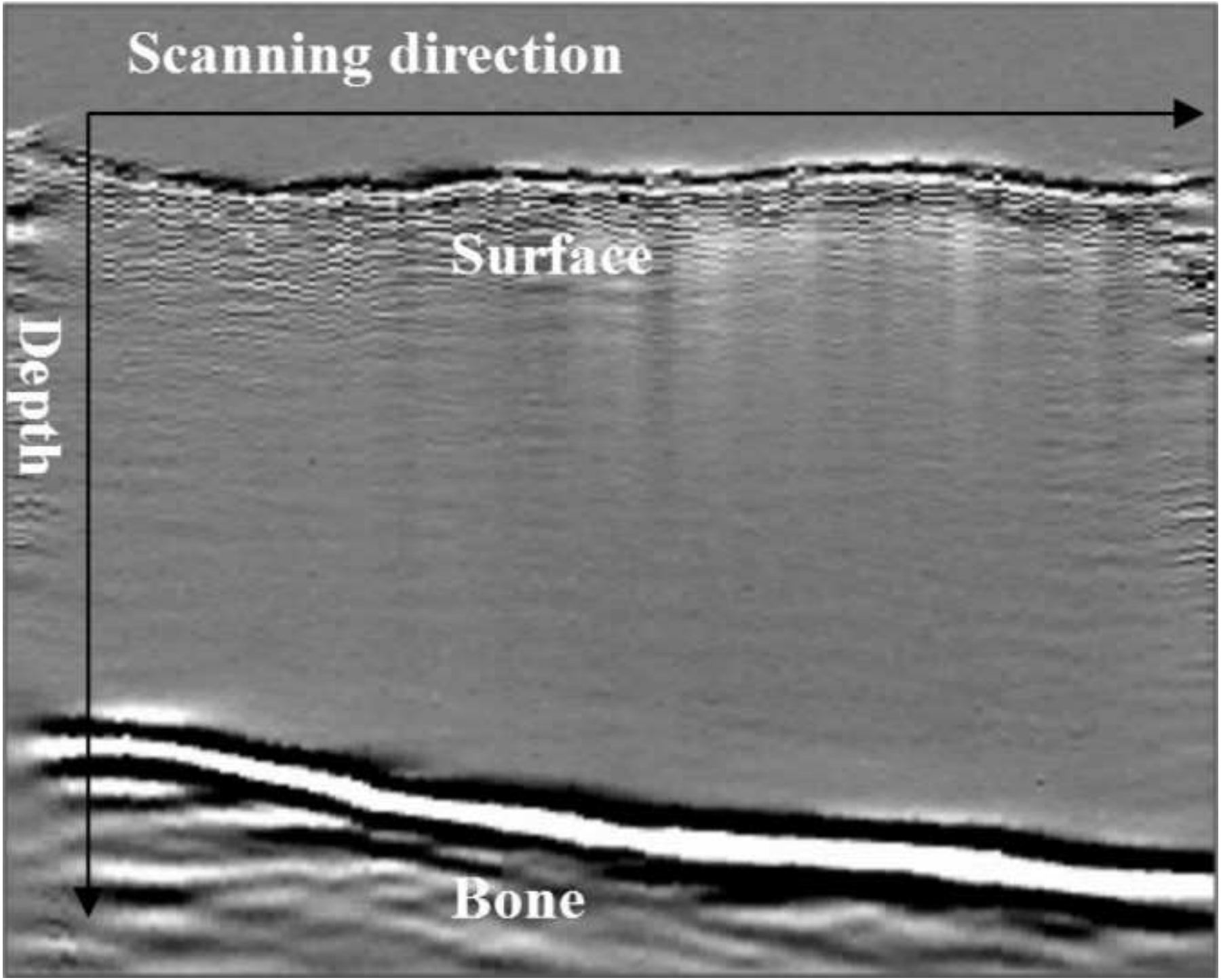

Figure 3

Click here to download high resolution image

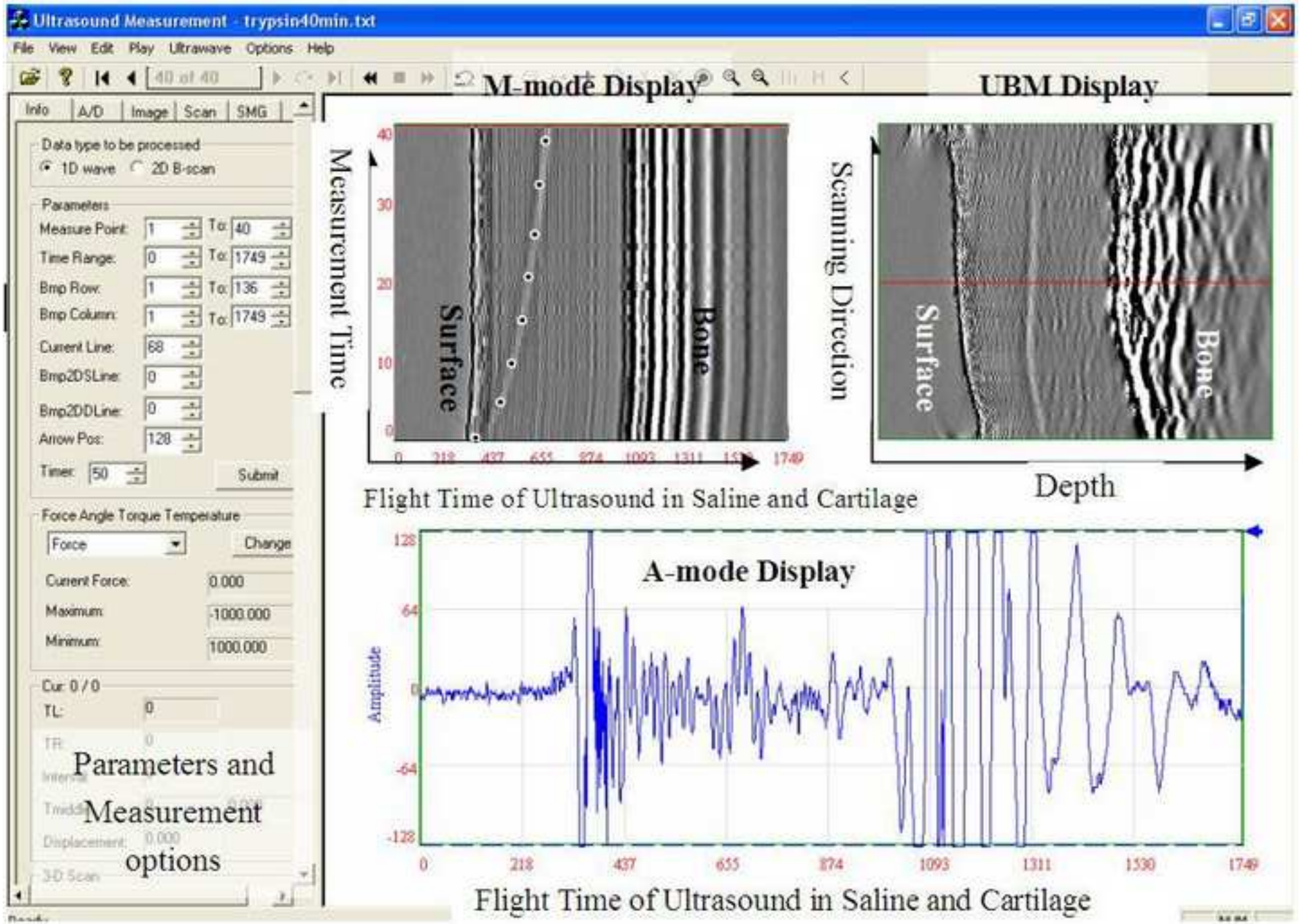

Figure 4a-b e-f i-j
Click here to download high resolution image

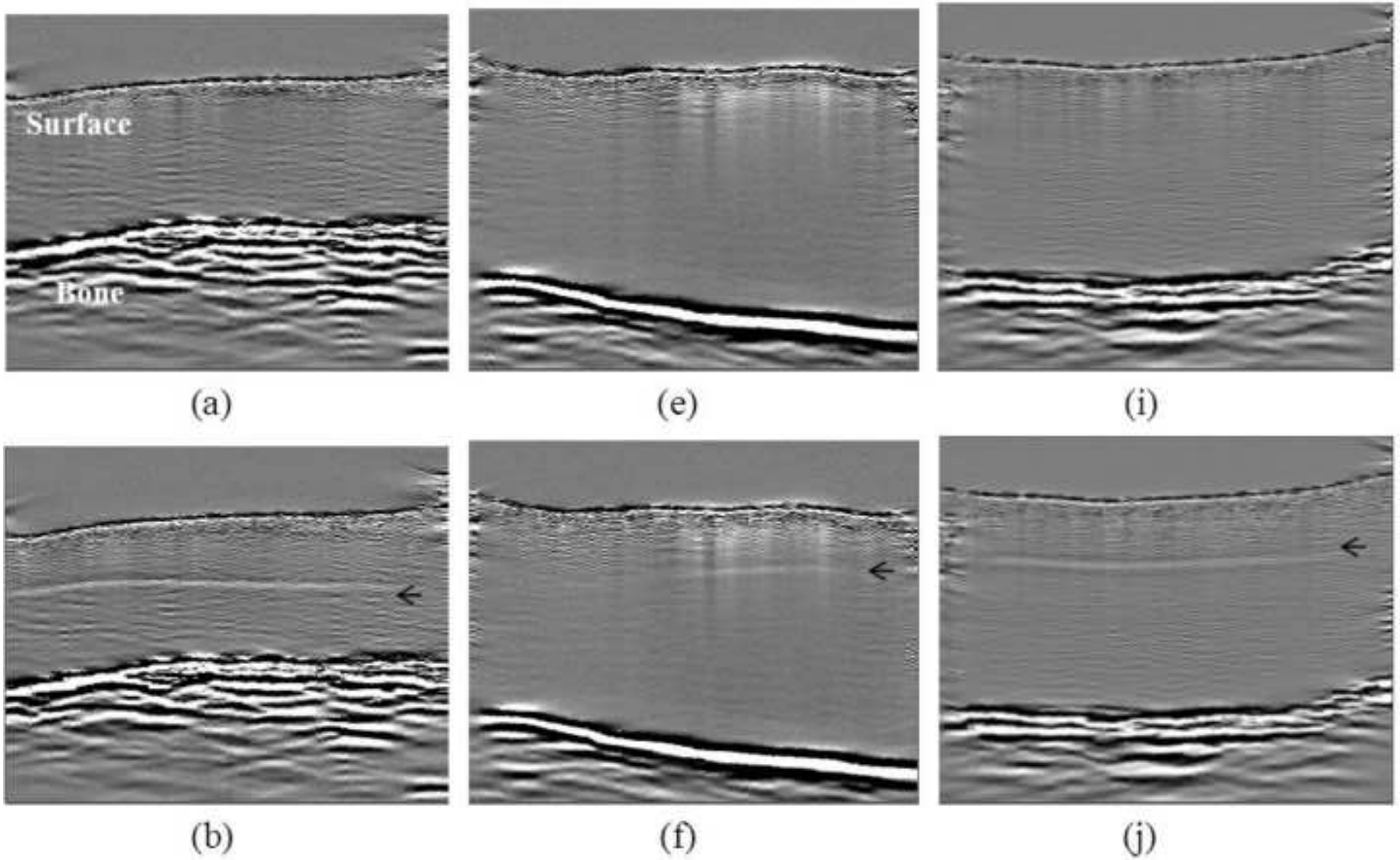

Figure 4c-d g-h k-l

Click here to download high resolution image

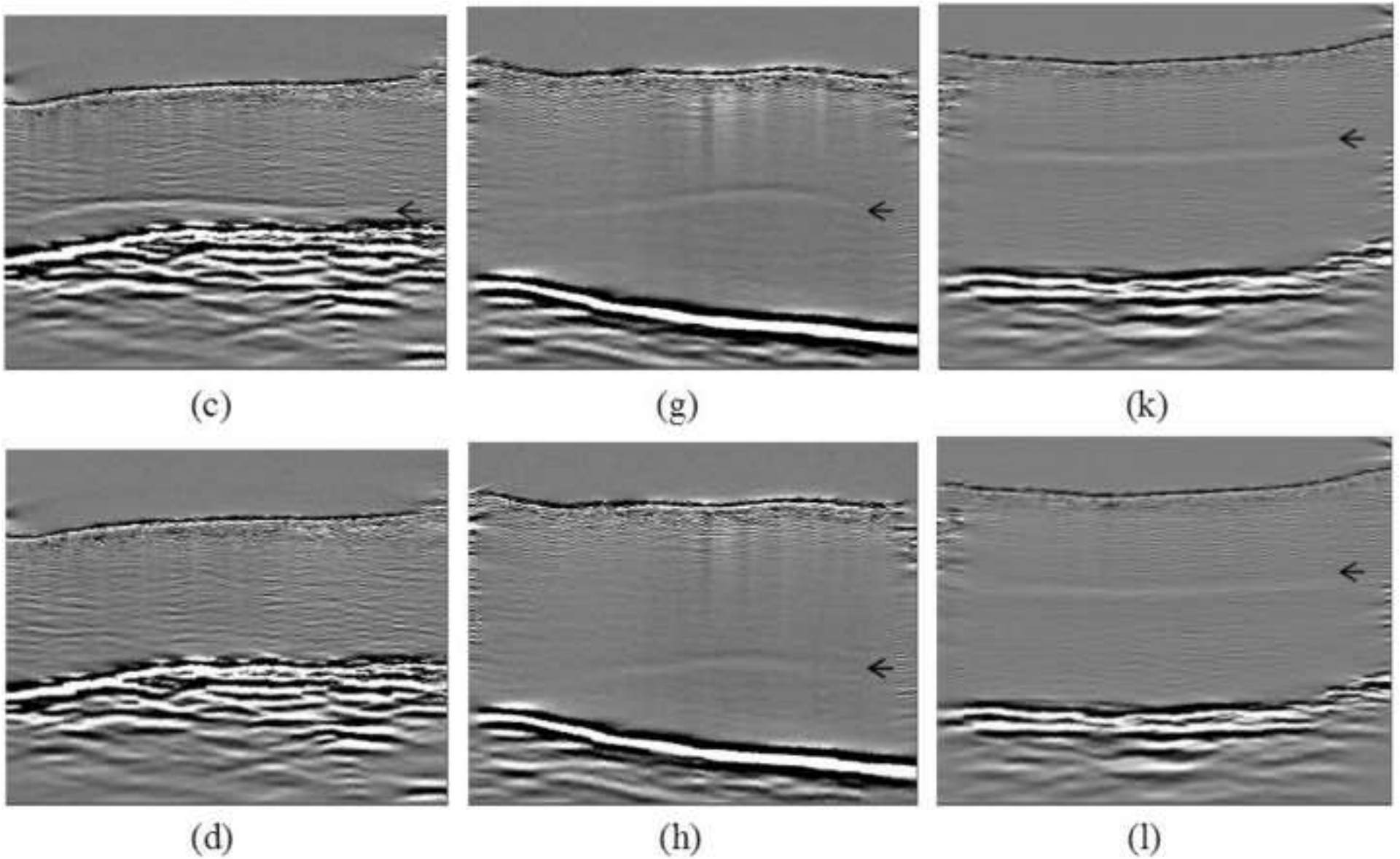

Figure 5a

Click here to download high resolution image

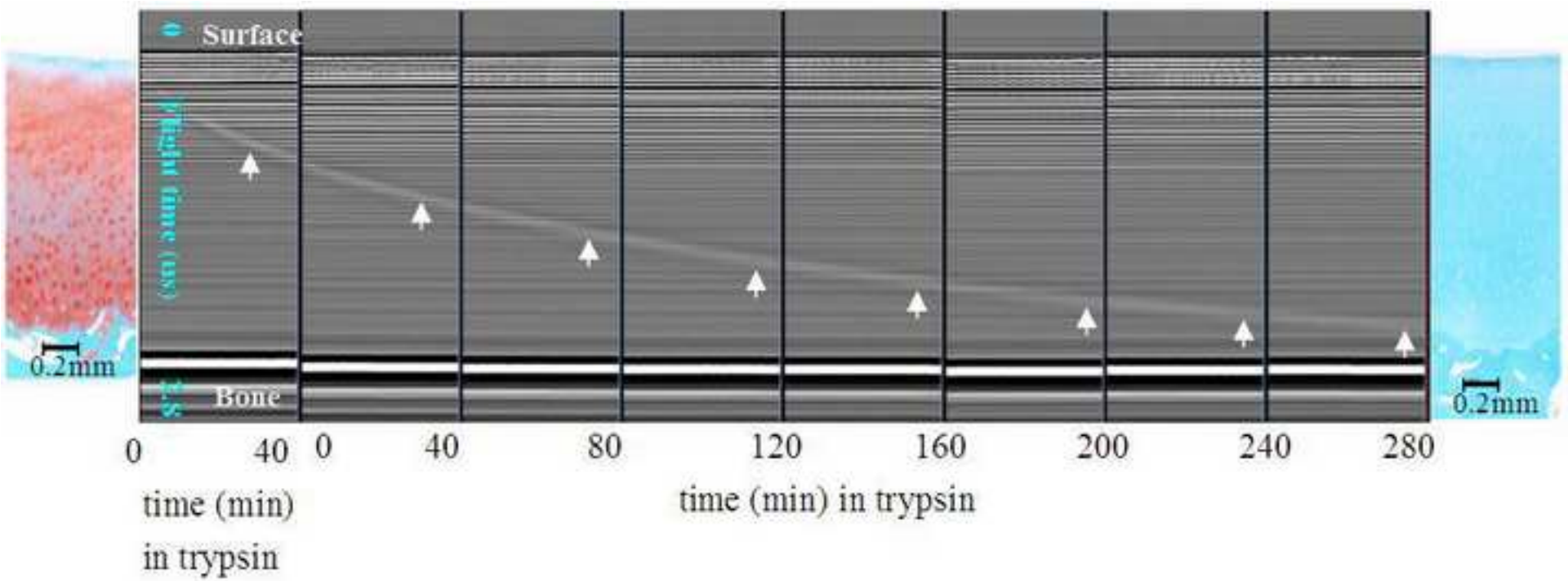

Figure 5b

Click here to download high resolution image

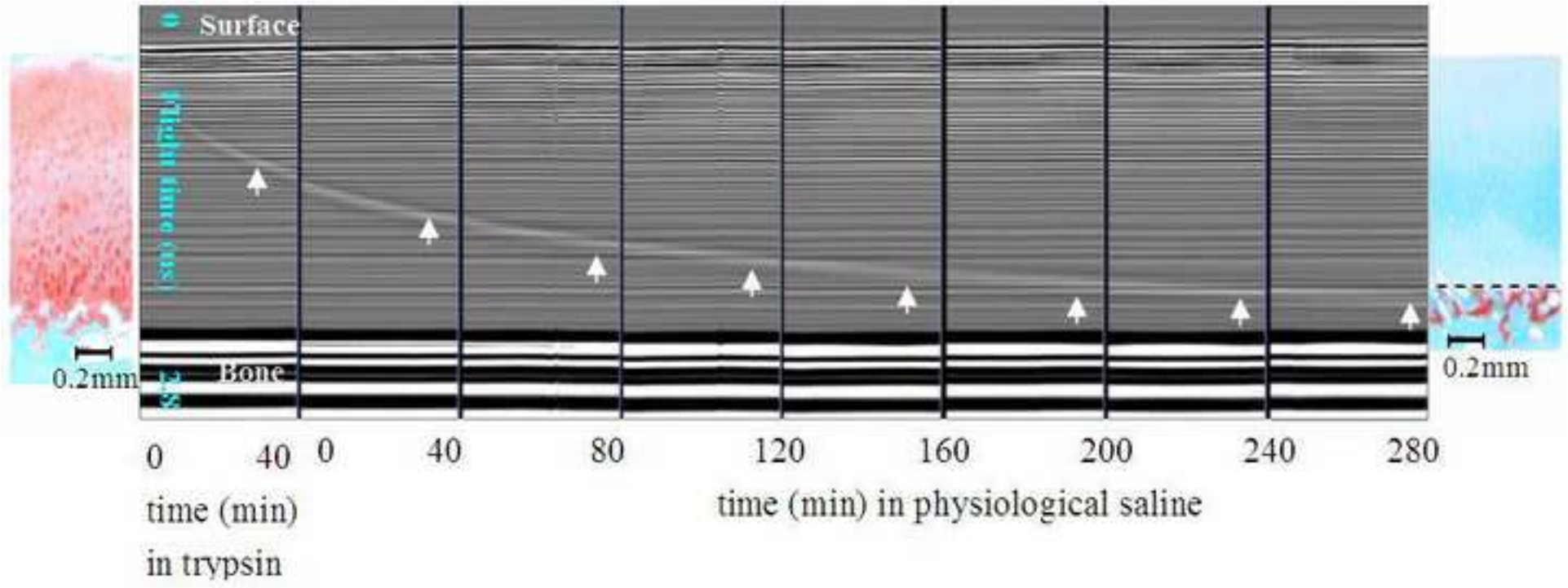

Figure 5c

Click here to download high resolution image

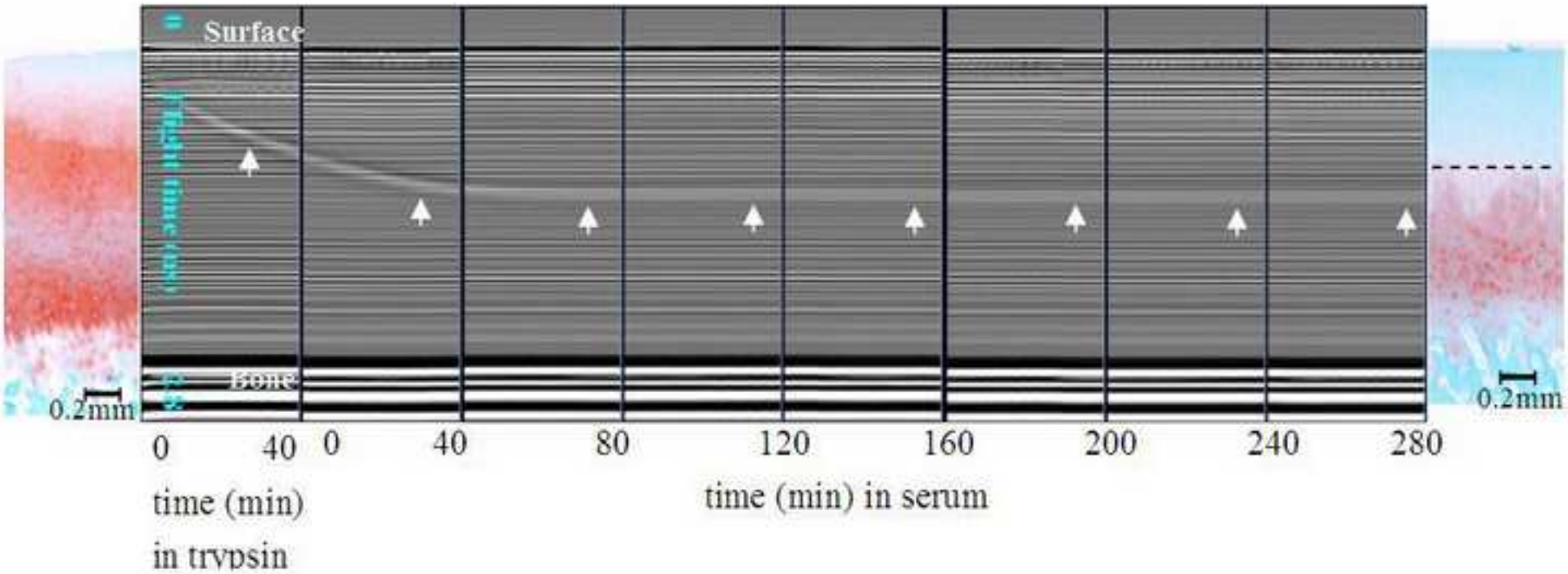

Figure 6

Click here to download high resolution image

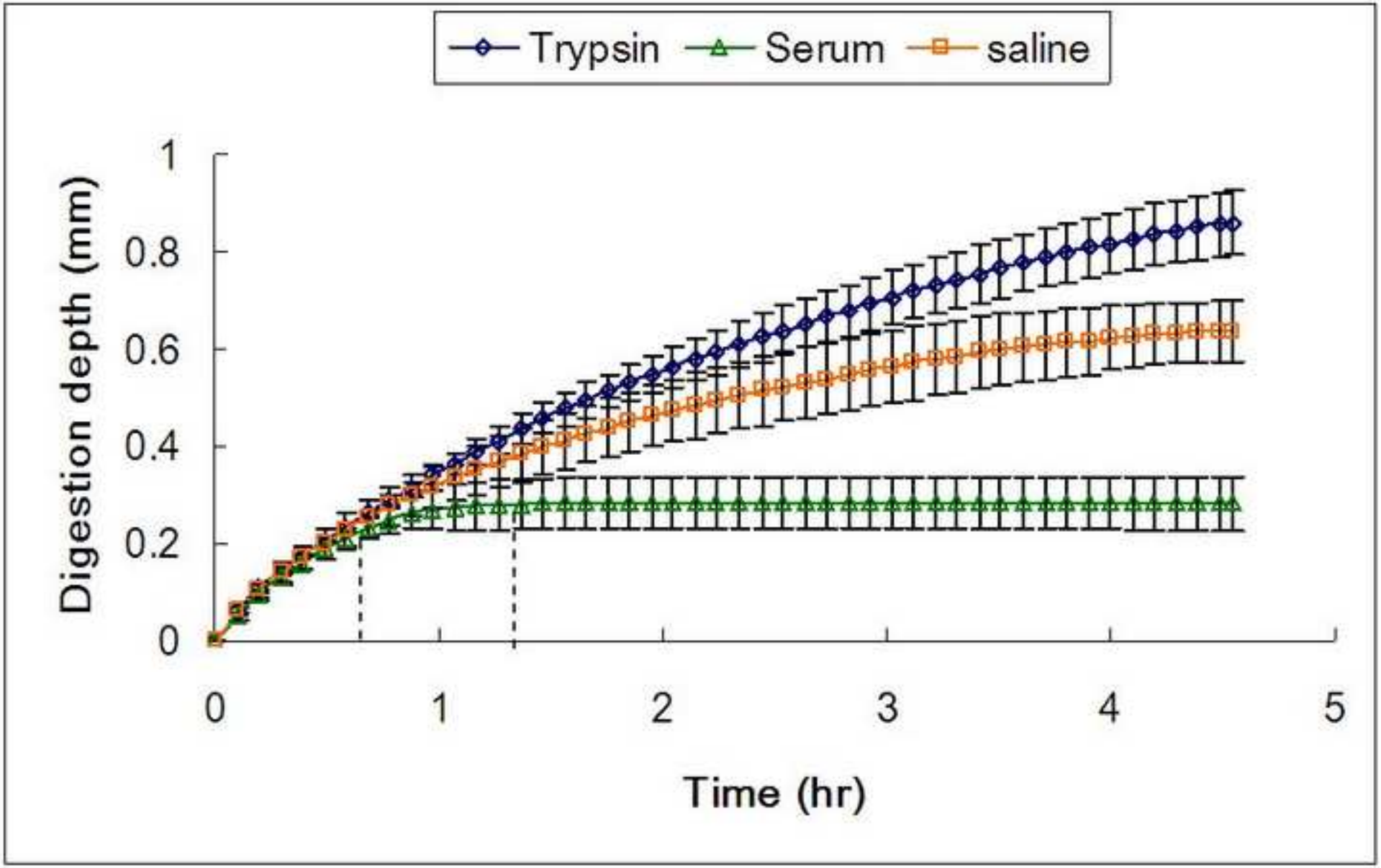

Table 1: The mean digestion fraction of the digested samples measured at the end of 40-min trypsin digestion and 280-min various treatments.

	40min-trypsin (n=9)	4h40min-trypsin (n=3)	4h40min-saline (n=3)	4h40min-serum (n=3)
Ultrasound measurement	0.38±0.08	0.88±0.06	0.83±0.19	0.50±0.02
Histological assessment	-	0.96±0.07	0.84±0.22	0.38±0.06